บทความวิชาการ

โครงสร้างและความเป็นแม่เหล็กของแบเรียมไททาเนต ที่เจือด้วยเหล็ก

นรวีร์ กาญจนวตี*

ได้รับบทความ: 16 กรกฎาคม 2561
ได้รับบทความแก้ไข: 28 สิงหาคม 2561
ยอมรับตีพิมพ์: 29 สิงหาคม 2561

บทคัดย่อ

มัลติเฟอร์โรอิกหรือสารที่แสดงสมบัติเฟอร์โรอิเล็กทริกและเฟอร์โรแมกเนติกพร้อมกัน เป็นสารที่ได้รับความสนใจอย่างสูง เนื่องจากสามารถนำไปใช้สร้างเทคโนโลยีใหม่เช่นหน่วยความจำสี่สถานะ แบเรียมไททาเนตเป็นสารที่มีสมบัติเฟอร์โรอิเล็กทริกที่รู้จักและมีการนำมาใช้อย่างกว้างขวางจึงเหมาะแก่การนำมาศึกษาสมบัติมัลติเฟอร์โรอิกด้วยการเจือด้วยธาตุโลหะทรานซิชันเพื่อก่อให้เกิดความเป็นแม่เหล็กขึ้นมาเนื่องจากเหล็กสามารถละลายได้ดีในแบเรียมไททาเนตทำให้มีโอกาสพบสารเจือปนที่มีความเป็นแม่เหล็กได้น้อย จึงเหมาะแก่การนำมาศึกษาในหัวข้อนี้ แบเรียมไททาเนตที่เจือด้วยเหล็กสามารถมีโครงสร้างได้ทั้งแบบเตตระโกนอลและเฮกซะโกนอลที่อุณหภูมิห้อง ซึ่งโครงสร้างนี้สามารถเปลี่ยนแปลงได้ด้วยการปรับอุณหภูมิและระยะเวลาในการอบ ปริมาณออกซิเจนขณะสังเคราะห์สาร รวมทั้งการเปลี่ยนความเข้มข้นของเหล็กที่ใช้เจือ นอกจากนี้ ปัจจัยดังกล่าวยังส่งผลต่อความเป็นแม่เหล็กของแบเรียมไททาเนตที่เจือด้วยเหล็กอีกด้วย มีการพบสมบัติเฟอร์โรแมกเนติกในแบเรียมไททาเนตที่เจือด้วยเหล็กที่อุณหภูมิห้องแต่ก็มีการพบสมบัติพาราแมกเนติกด้วยเช่นกัน โดยแบบจำลองทางแม่เหล็ก เช่น การแลกเปลี่ยนอย่างยิ่งยวด (superexchange) และการจับคู่ผ่านตำแหน่งที่ว่างของออกซิเจน (oxygen vacancy-mediated coupling) ได้รับการนำเสนอเพื่อใช้อธิบายสมบัติเฟอร์โรแมกเนติกที่เกิดขึ้นนี้ แต่ในขณะเดียวกันก็มีการรายงานการพบความเป็นแม่เหล็กที่เกิดจากเหล็กที่ไม่เข้าไปก่อพันธะในแบเรียมไททาเนต และการเกิดสมบัติเฟอร์โรแมกเนติกที่มาจากความเครียดในตัวสารเอง

คำสำคัญ: แบเรียมไททาเนตที่เจือด้วยเหล็ก โครงสร้างผลึก สมบัติแม่เหล็ก

ภาควิชาฟิสิกส์ คณะวิทยาศาสตร์ จุฬาลงกรณ์มหาวิทยาลัย
*ผู้นิพนธ์ประสานงาน, email: noravee.k@chula.ac.th

Polymorphism and Magnetism in Fe-doped $BaTiO_3$

Noravee Kanchanavatee*

Received: 16 July 2018
Revised: 28 August 2018
Accepted: 29 August 2018

ABSTRACT

Multiferroicity, a spontaneous emergence of ferroelectricity and ferromagnetism in a material, is a greatly desired property thanks to its technological aspirations, such as four-state memory. A well-known ferroelectric material, barium titanate offers a platform to study multiferroicity by doping transition metals to induce ferromagnetism. Iron is an appealing choice for chemical substitution due to its high solubility in $BaTiO_3$. Thus, spurious ferromagnetic impurity phases are less likely to precipitate. Fe-doped $BaTiO_3$ can adopt either tetragonal or hexagonal structure at room temperature. The structure can be tuned by fabrication temperature, processing duration, oxygen pressure and iron doping concentrations. These parameters also have an impact on the magnetic behavior of Fe-substituted $BaTiO_3$. In addition to room temperature ferromagnetism, paramagnetism was also found in Fe-doped $BaTiO_3$. While multiple models, such as superexchange, double exchange, oxygen vacancy-mediated coupling, were proposed for the magnetic behavior, Fe metal clusters and strain-induced extrinsic ferromagnetism were also reported.

Keywords: Fe-doped Barium titanate, polymorphism, magnetism

Department of Physics, Faculty of Science, Chulalongkorn University
*Corresponding author, email: noravee.k@chula.ac.th

Introduction

Ferroelectricity is defined as a spontaneous polarization switchable by an applied electric field. Similarly, a spontaneous magnetization switchable by an external magnetic field is a unique characteristic of ferromagnetism. Materials exhibit both of the phenomena are known as multiferroic materials. Such materials have attracted a multitude of attention thanks to their technological potentials, such as transducers, magnetic field sensors, and four-state memory [1]. Even though multiferroic materials do exist in nature, they are too scarce [2]. Therefore, numerous materials have been studied in search of the elusive property. One of the candidates is barium titanate ($BaTiO_3$ or BTO), a well-known ferroelectric material, which has been used in capacitors and piezoelectric applications [3]. BTO is intrinsically diamagnetic owing to unfilled or full orbitals of Ba^{2+}, Ti^{4+}, and O^{2+}. However, induced ferromagnetism was predicted for transition metal-doped B+TO, especially Fe, Mn, and Cr substitution [4, 5]. Note that Ba^{2+} ionic radius (1.61 Å) is more than twice as large as those of Ti^{4+} (0.605 Å), Fe^{3+} (0.645 Å), Mn^{4+} (0.53 Å), and Cr^{3+} (0.615 Å) [6]. Therefore, the dopant ions prefer to occupy Ti-site [7]. Room temperature ferromagnetism was observed in BTO doped with transition metals, e.g. Fe, Mn, Cr, and Co [8]. Nevertheless, the nature of the magnetic order is still disputable. The fabricated ferromagnetism is believed by some to be intrinsic while others suspect that it is a result of elemental clusters or spurious ferromagnetic phases, often found in dilute magnetic oxides [9]. Because of the high solubility of Fe in BTO [10], secondary phases such as γ-Fe_2O_3 and Fe_3O_4 were rarely detected in Fe-doped BTO, making it an intriguing alternative for multiferroic materials. The magnetic behavior in Fe-doped BTO has intricate correlations with the structure. Hence, the focus of this review is on the structural and magnetic properties as well as their interactions.

Polymorphism

BTO is a perovskite with general formula of ABO_3, where Ba occupies A-site at the corners of the cube, Ti occupies B-site at the center, and O locates at the face centers of the cell (Fig. 1(a)). Furthermore, Ti and O constitute a TiO_6 corner-sharing octahedron. As a polymorphic material, BTO undergoes multiple phase transitions: hexagonal ($P6_3/mmc$) $\xrightarrow{1460°C}$ cubic ($Pm\bar{3}m$) $\xrightarrow{125\,°C}$ tetragonal ($P4mm$) $\xrightarrow{0\,°C}$ orthorhombic (Amm2) $\xrightarrow{-90\,°C}$ rhombohedral (R3m) [11, 12]. The hexagonal structure belongs to the 6H polytype whereas the others can be categorized as the 3C polytype. In other words, the three structures at lower temperatures can be considered as distortions of the cubic phase; for instance, the Ti at the center of the octahedron, which is shifted slightly off-center in the tetragonal phase. On the other hand, the hexagonal

structure is markedly different from the 3C polytype. As can be seen in Fig. 1(b), the unit cell of the 6H-BTO consists of stacking BaO_3 layers and, more importantly, two Ti-sites. Ti(1) forms corner-sharing octahedra similar to the ones in the 3C-BTO whereas Ti(2) forms Ti_2O_9 face-sharing octahedra [13]. Unlike the tetragonal phase, which is stable at room temperature, the hexagonal phase normally is stable in air at 1460°C or more [14]. However, there are 3 methods of stabilizing the hexagonal structure at room temperature [15]. The first one is to quench the sample or cool it down very rapidly [14]. The second one is annealing in a reducing atmosphere [13]. Doping with some transition metals, such as Fe, is the third one [16]. To determine the crystal structure of Fe-doped BTO at room temperature, several parameters have to be taken into account. Two of the most important parameters are processing temperatures and iron concentrations. As can be seen in Fig. 2, the hexagonal structure was found at high annealing temperatures and high Fe concentrations while the tetragonal phase was detected at low annealing temperatures. A mixture of the tetragonal and hexagonal structures was often observed in an intermediate processing temperature range. Synthesis methods and conditions, such as heat treatment time and oxygen pressure, are also important parameters to take into consideration. For conventional solid state reaction, it is necessary for the heat treatment temperature to be high, approximately more than 1200°C [17]. Around this temperature, Fe-doped BTO is detected in the tetragonal phase at very low doping concentration, while the mixed phase and the hexagonal phase are found at the intermediate and high doping concentrations, respectively [18]. Thus, chemical methods like sol-gel and hydrothermal have an advantage in assisting the formation of the tetragonal phase [19]. It has also been observed that increasing the heat treatment temperature and annealing time promotes the hexagonal phase [20] whereas reduced oxygen pressure may lead to phase separation [21]. Stoichiometry between Ba and Ti+Fe also plays a role in determining the phase structure [22].

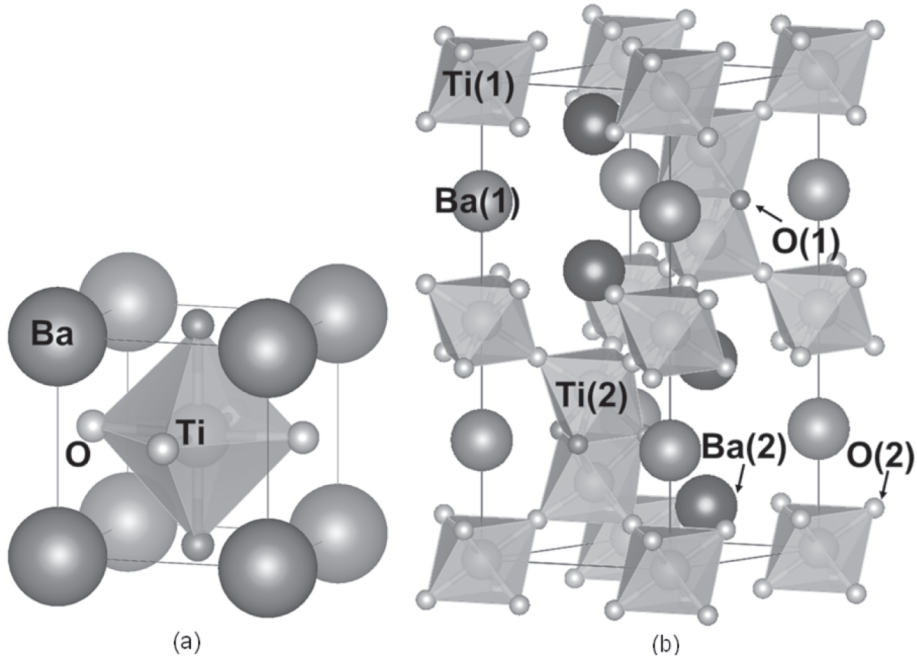

Figure 1 The crystal structure of (a) 3C-BTO and (b) 6H-BTO.

A widely accepted factor attributed to the formation of the hexagonal BTO is oxygen vacancies [23]. As the concentration of the oxygen vacancies increases, the structure eliminates the vacancies by having face-sharing octahedra instead of just corner-sharing ones as in the 3C polytype [22]. However, due to the short distance between Ti^{4+} in Ti_2O_9 face-sharing octahedra (2.69 Å) [13], the high electrostatic repulsion makes the structure unstable at room temperature. Therefore, reduction of Ti^{4+} to Ti^{3+} by annealing in a reducing atmosphere or substitution by Fe^{3+} decreases the repulsion and stabilizes the structure at room temperature. The effect of the electrostatic force can also be lessened by overlapping of the *d*-orbitals [22]. Jahn-teller effect from Fe^{4+} was proposed as another driving force of the structural phase transition [12]. Even though most Fe valences found in the Fe-doped BTO are 3+, there are several cases of 4+ detections in samples annealed in an oxygen atmosphere [14] or in air [24]. The crystal structure, oxygen vacancies, and oxidation states and site of occupancy of Fe ions play a crucial role in understanding the magnetic exchange interactions, and therefore the magnetic properties of the Fe-substituted BTO.

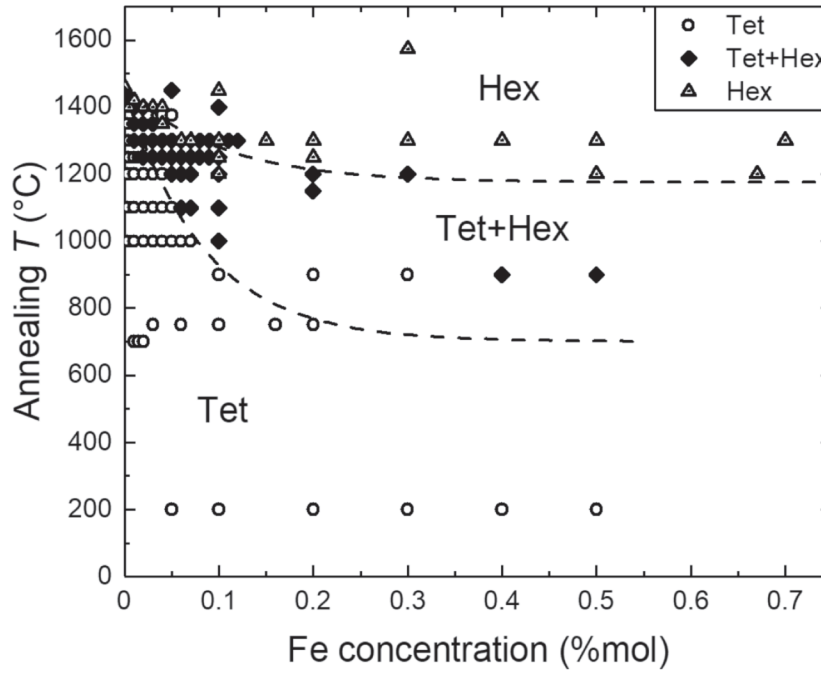

Figure 2 Annealing temperature vs Fe concentration phase diagram of Fe-doped BTO. The dash lines are provided to show the separations between the tetragonal (Tet), hexagonal (Hex), and mixed phases (Tet+Hex). Data points were extracted from [7,10,14,18–35] and references therein.

Magnetism

Studies on magnetic properties of the Fe-doped BTO yield debatable and controversial results. Several magnetic behaviors were detected, including paramagnetism [20], ferrimagnetism [36], and ferromagnetism with ordered moments and Curie temperatures ranging from 0.001 [37] to 0.58 [38] μ_B/Fe and 460 [39] °C to 810 [18] °C, respectively. Since the structural phase transition is sensitive to fabrication techniques and conditions, BTO doped with a similar Fe concentration often exhibit different structures and magnetic orderings. Fig. 3 shows a compendium of the average magnetic moments in different structures with various fabrication conditions as a function of Fe concentrations. Note that the magnitude of the magnetic moment was estimated from the saturation magnetization subtracted by the linear paramagnetic component. Interestingly, the thin film samples exhibit larger ordered magnetic moment comparing to that of the bulk samples at the same Fe concentration, indicating a possible

different exchange mechanisms for the magnetic behaviors. In addition, the oxygen vacancies are also significant for the magnetism in Fe-doped BTO. At low Fe concentrations, the saturation magnetization is enhanced by annealing the samples in vacuum, and decreased for samples annealed with oxygen flow [34] whereas the opposite behavior is observed at high Fe concentrations [40]. This contradiction points to distinct exchange interactions in BTO doped with a small and large amount of Fe. Additionally, oxygen vacancies change the local structure of Fe. Removal of one oxygen ion transforms an octahedron to a pentahedron. Moreover, the oxidation state of Fe ion is associated with oxygen vacancies. To preserve the electroneutrality, zero, one half, and one oxygen vacancies, created as Ti^{4+}, is substituted by Fe^{4+}, Fe^{3+}, and Fe^{2+}, respectively. Ti^{4+} can be reduced to Ti^{3+} by oxygen vacancies, as well. Both of the local environment and the oxidation state of Fe ion are critical to magnetic exchange interactions. For instance, the superexchange between octahedral Fe^{3+} is antiferromagnetic, but the interaction of pentahedral Fe^{3+} is ferromagnetic [37]. On the other hand, two octahedral Fe^{4+} give rise to a ferromagnetic superexchange [41]. Conversely, the induction of ferromagnetism may not be directly related to the oxygen vacancies. It was found that ferromagnetic order was induced by redistribution of Fe ions from a random distribution among Ti(1) and Ti(2) sites to Ti(2) preference creating Fe_2O_9 dimers from the face-sharing octahedral. Prolonged heat treatment is believed to be the trigger of the redistribution [42, 43].

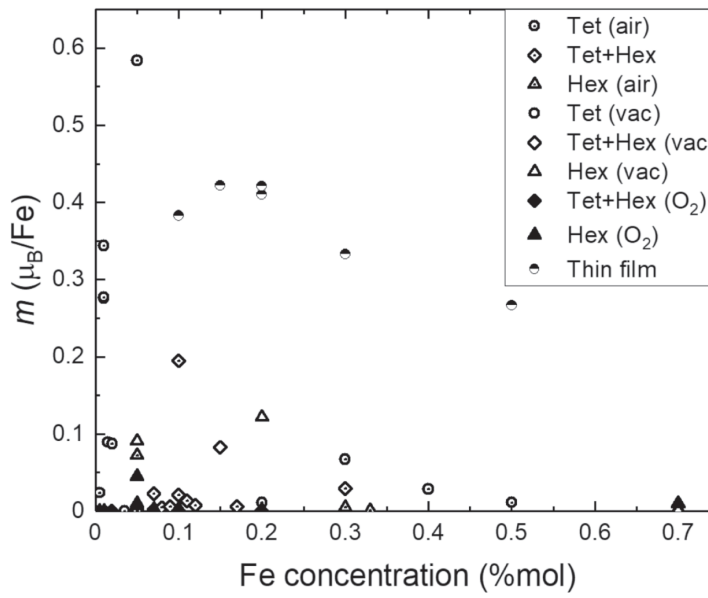

Figure 3 Average magnetic moment of the tetragonal, hexagonal, and mixed phases and synthesis atmosphere (air, vacuum, and oxygen) vs Fe concentration of Fe-doped BTO. Thin film samples were in the tetragonal phase and grown using pulsed-laser deposition technique. Data were extracted from [17–20, 25, 29, 32, 34, 36–53].

Even with numerous investigations, the origin of ferromagnetism in Fe-doped BTO remains elusive. In many dilute magnetic oxides, dopant segregations or spurious ferromagnetic phases are often identified as sources of the magnetic signals [9]. Those cases are rare for BTO substituted with iron thanks to the high solubility. Thus, most studies claimed the results as intrinsic, and a variety of models has been proposed including superexchange [37, 41] and double exchange [54]. However, superexchange and double exchange are short-range. Several longer-range ferromagnetic exchange interactions were suggested, such as electron-mediated Zener-type RKKY interaction [38, 55] and oxygen vacancy-mediated coupling of Fe ions forming bound magnetic polarons which overlap to create a spin-split impurity band [56]. A direct exchange between Fe in Fe_2O_9 dimers is considered as a possible mechanism of generating ferromagnetic behavior in the hexagonal phase [45, 57]. A compilation of exchange interactions suggested for Fe-doped BTO can be seen in Table 1. It is also possible that a combination of magnetic exchange interactions is responsible for the ordering in Fe-doped BTO since multiple magnetic behaviors were observed.

Table 1 Exchange interactions of Fe-doped BTO with different structures, Fe concentrations, and annealing atmospheres. Tet, Hex, vac, and V_O denote the tetragonal structure, hexagonal structure, vacuum, and oxygen vacancies, respectively.

Structure	concentration	atmosphere	Exchange interaction	ref
Tet	0.5-0.75	vac	superexchange Fe^{4+}-O^{2}-Fe^{4+}	[41]
	0.15-0.5	vac	superexchange low spin Fe^{4+}-O^{2}-high spin Fe^{3+}	[44]
	0.05	air	electron-mediated Zener-type RKKY	[38]
	0.005	air	superexchange Ti^{3+}-V_O-Ti^{3+}	[17]
	0.01-0.02	air	superexchange Fe^{3+}-V_O- Fe^{3+}	[48]
	0.1-0.6	air	double exchange Fe^{3+}-O^{2}-Fe^{4+}	[54]
Hex	0.3-0.7	air	superexchange Fe^{3+}-O^{2}-Fe^{3+}	[37]
	0.33	air	superexchange Fe^{3+}-VO- Fe^{3+}	[47]
	0.05-0.07	O_2	direct exchange Fe^{3+}-Fe^{3+}	[45]
	0.7	O_2	superexchange Fe^{4+}-O^{2}-Fe^{4+}	[40]

Although most researchers recognize that the ferromagnetism is intrinsic, several support the opposite view of extrinsic magnetism. Fe metal cluster was detected in 100 ppm Fe doping in BTO [33] and 5 mol% Fe-doped BTO annealed under a reducing atmosphere [21]. Recently, it is reported that ferromagnetism in the hexagonal phase is extrinsic and caused by

sparse-strain induced the tetragonal phase [58]. As discussed in this review, the study of the underlying mechanism to the magnetic ordering in Fe-doped BTO is still an ongoing topic. To shed light on the origin of the ferromagnetism, comprehensive and thorough studies of the dependence of fabrication conditions, including annealing temperature, time, and oxygen pressure, on the structural and magnetic properties is required.

Conclusion

Fe-doped BTO is a promising candidate for a multiferroic material thanks to the ferroelectric property of the pure BTO and the induced ferromagnetism from the doping Fe. Nevertheless, the results from many studies are still inconsistent and controversial. This is due to the fact that BTO is polymorphic, and Fe-doped BTO can be in either the tetragonal or the hexagonal or the mixed phase depending on the synthesis methods and conditions. Several magnetic exchange interactions were proposed to explain the induce magnetism in Fe-substituted BTO, but the possibility of spurious impurity phases cannot be completely ignored.

References

1. Eerenstein, W., Mathur, N. D., & Scott, J. F. (2006). Multiferroic and magnetoelectric materials. *Nature, 442,* 759–765.
2. Hill, N. A. (2000). Why are there so few magnetic ferroelectrics? *The Journal of Physical Chemistry B, 104*(29), 6694–6709.
3. Vijatović, M. M., Bobić, J. D., & Stojanović, B. D. (2008). History and challenges of barium titanate: Part I. *Science of Sintering, 40*(3), 235-244.
4. Nakayama, H., & Katayama-Yoshida, H. (2001). Theoretical prediction of magnetic properties of $Ba(Ti_{1-x}M_x)O_3$ (M = Sc, V, Cr, Mn, Fe, Co, Ni, Cu). *Japanese Journal of Applied Physics, 40*(12B), L1355–L1358.
5. Apostolova, I. N., Apostolov, A. T., Golrokh Bahoosh, S., & Wesselinowa, J. M. (2013). Origin of ferromagnetism in transition metal doped $BaTiO_3$. *Journal of Applied Physics, 113*(20), 203904-1–203904-4.
6. Shannon, R. D. (1976). Revised effective ionic radii and systematic studies of interatomic distances in halides and chalcogenides. *Acta Crystallographica Section A, 32*(5), 751–767.
7. Lin, F. & Shi, W. (2012). Effects of doping site and pre-sintering time on microstructure and magnetic properties of Fe-doped $BaTiO_3$ ceramics. *Physica B: Condensed Matter, 407*(3), 451–456.

8. Verma, K. C. & Kotnala R. K. (2016). Multiferroic approach for Cr, Mn, Fe, Co, Ni, Cu substituted $BaTiO_3$ nanoparticles. *Material Research Express, 3,* 055006-1-055006-13.

9. Coey, J. M. D. & Chambers, S. A. (2008). Oxide dilute magnetic semiconductors-Fact or Fiction? *MRS Bulletin, 33,* 1053–1058.

10. Keith, G. M., Rampling, M. J., Sarma, K., Mc. Alford, N., & Sinclair, D. C. (2004). Synthesis and characterisation of doped 6H-$BaTiO_3$ ceramics. *Journal of the European Ceramic Society, 24*(6), 1721–1724.

11. Glaister R. M. & Kay H. F. (1960). An investigation of the cubic-hexagonal transition in barium titanate. *Proceedings of the Physical Society, 76*(5), 763-771.

12. Böttcher, R., Langhammer, H. T., Müller, T., & Abicht, H. -P. (2008). 3C–6H Phase transition in $BaTiO_3$ induced by Fe ions: An electron paramagnetic resonance study. *Journal of Physics: Condensed Matter, 20*(50), 505209-1–505209-8.

13. Sinclair, D. C., Skakle, J. M. S., Morrison, F. D., Smith, R. I., & Beales, T. P. (1999). Structure and electrical properties of oxygen-deficient hexagonal $BaTiO_3$. *Journal of Materials Chemistry, 9*(2), 1327–1331.

14. Grey, I. E., Li, C., Cranswick, L. M. D., Roth, R. S., & Vanderah, T. A. (1998). Structure analysis of the 6H–Ba(Ti, Fe^{3+}, Fe^{4+})$O_{3-\delta}$ solid solution. *Journal of Solid State Chemistry, 321*(135), 312–321.

15. Keith, G. M., Sarma, K., Alford, N. M. C. N., & Sinclair, D. C. (2004). Electrical properties of 6H-$BaTi_{0.95}M_{0.05}O_{3-\delta}$ ceramics where *M* = Mn, Fe, Co, and Ni. *Journal of Electroceramics, 13*, 305–309.

16. Mashkina, E., McCammon, C., & Seifert, F. (2004). A Mössbauer study of oxygen vacancy and cation distribution in 6H-$BaTi_{1-x}Fe_xO_{3-x/2}$ *Journal of Solid State Chemistry, 177*(1), 262–267.

17. Dang, N. V., Thanh, T. D., Hong, L. V., Lam, V. D., & Phan, T. -L. (2011). Structural, optical and magnetic properties of polycrystalline $BaTi_{1-x}Fe_xO_3$ ceramics. *Journal of Applied Physics, 110*(4), 043914-1–043914-7.

18. Dang, N. V., Nguyen, H. M., Chuang, P. -Y., Zhang, J. -H., Thanh, T. D., Hu, C. -W., Chen, T. -Y., Yang, H. -D., Lam, V. D., Lee, C. -H., & Hong, L. V. (2012). Structure and magnetism of $BaTi_{1-x}$ $Fe_xO_{3-\delta}$ multiferroics. *Journal of Applied Physics, 111*(7), 07D915-1–07D915-3.

19. Yang, L., Qiu, H., Pan, L., Guo, Z., Xu, M., Yin, J., & Zhao, X. (2014). Magnetic properties of $BaTiO_3$ and $BaTi_{1-x}M_xO_3$ (*M* = Co, Fe) nanocrystals by hydrothermal method. *Journal of Magnetism and Magnetic Materials, 350,* 1–5.

20. Qiu, S. Y., Li, W., Liu, Y., Liu, G. H., Wu, Y. Q., & Chen, N. (2010). Phase evolution and room temperature ferroelectric and magnetic properties of Fe-doped $BaTiO_3$ ceramics. *Transactions of Nonferrous Metals Society of China (English Edition), 20*(10), 1911–1915.
21. Chakraborty, T., Meneghini, C., Aquilanti, G., & Ray, S. (2014). Investigating the development of spurious magnetism in single crystalline $BaTi_{0.95}M_{0.05}O_{3-\delta}$ with high δ by local structural probes. *Journal of Physics Condensed Matter, 26*(19), 196001-1–196001-7.
22. Jayanthi, S. & Kutty, T. R. N. (2008). Dielectric properties of 3d transition metal substituted $BaTiO_3$ ceramics containing the hexagonal phase formation. *Journal of Materials Science: Materials in Electronics, 19*(7), 615–626.
23. Chakraborty, T., Ray, S., & Itoh, M. (2011). Defect-induced magnetism: Test of dilute magnetism in Fe-doped hexagonal $BaTiO_3$ single crystals. *Physical Review B-Condensed Matter and Materials Physics, 83*(14), 1–8.
24. Nguyen, H. M., Dang, N. V., Chuang, P.Y., Thanh, T.D., Hu, C.W., Chen, T.Y., Lam, V. D., Lee, C. -H., & Hong, L. V. (2011). Tetragonal and hexagonal polymorphs of $BaTi_{1-x}Fe_xO_{3-\delta}$ multiferroics using x-ray and Raman analyses. *Applied Physics Letters, 99*(20), 202501-1–202501-3.
25. Masó, N., Beltrán, H., Cordoncillo, E., Escribano, P., & West, A. R. (2006). Electrical properties of Fe-doped $BaTiO_3$. *Journal of Materials Chemistry, 16*(17), 1626–1633.
26. Banerjee, A., Das, A., Das, D., Saha, A., & Sarkar, S. (2018). Mössbauer study of Fe-doped $BaTiO_3$ of different grain sizes induced by Ball Mill technique. *Journal of Magnetism and Magnetic Materials, 449,* 180–184.
27. Langhammer, H. T., Müller, T., Walther, T., Böttcher, R., Hesse, D., Pippel, E., & Ebbinghaus, S. G. (2016). Ferromagnetic properties of barium titanate ceramics doped with cobalt, iron, and nickel. *Journal of Materials Science, 51*(23), 10429–10441.
28. Luo, B., Wang, X., Tian, E., Song, H., Zhao, Q., Cai, Z., Feng, W., & Li, L. (2018). Giant permittivity and low dielectric loss of Fe doped $BaTiO_3$ ceramics: Experimental and first-principles calculations. *Journal of the European Ceramic Society, 38*(4), 1562–1568.
29. Gheorghiu, F., Simenas, M., Ciomaga, C.E., Airimioaei, M., Kalendra, V., Banys, J., Dobromir M., Tascu S., & Mitoseriu L. (2017). Preparation and structural characterization of Fe-doped $BaTiO_3$ diluted magnetic ceramics. *Ceramics International, 43*(13), 9998–10005.
30. Chikada, S., Hirose, K., & Yamamoto, T. (2010). Analyze of local environment of Fe ion in hexagonal $BaTiO_3$. *Japanese Journal of Applied Physics, 49,* 091502-1–091502-3.
31. Rajan, S., Gazzali, P. M. M., & Chandrasekaran, G. (2017). Impact of Fe on structural modification and room temperature magnetic ordering in $BaTiO_3$. *Spectrochimica Acta-Part A: Molecular and Biomolecular Spectroscopy, 171,* 80–89.

32. Kundu, T. K., Jana, A., & Barik, P. (2008). Doped barium titanate nanoparticles. *Bulletin of Materials Science, 31*(3), 501–505.

33. Khirade, P. P., Birajdar, S. D., Raut, A. V., & Jadhav, K. M. (2016). Multiferroic iron doped $BaTiO_3$ nanoceramics synthesized by sol-gel auto combustion: Influence of iron on physical properties. *Ceramics International, 42*(10), 12441–12451.

34. Dutta, D. P., Roy, M., Maiti, N., & Tyagi, A. K. (2016). Phase evolution in sonochemically synthesized Fe^{3+} doped $BaTiO_3$ nanocrystallites: Structural, magnetic and ferroelectric characterisation. *Physical Chemistry Chemical Physics, 18*(14), 9758–9769.

35. Figueiras, F. G., Amorim, C. O., Amaral, J., Moreira, J. A., Tavares, P. B., Alves, E., & Amaral, V. S. (2016). Magnetoelectric effect probe through ppm Fe doping in $BaTiO_3$. *Journal of Alloys and Compounds, 661,* 495–500.

36. Maier, R., Cohn, J. L., Neumeier, J. J., & Bendersky, L. A. (2001). Ferroelectricity and ferrimagnetism in iron-doped $BaTiO_3$. *Applied Physics Letters, 78*(17), 2536–2538.

37. Lin, F., Jiang, D., Ma, X., & Shi, W. (2008). Influence of doping concentration on room-temperature ferromagnetism for Fe-doped $BaTiO_3$ ceramics. *Journal of Magnetism and Magnetic Materials, 320*(5), 691–694.

38. Xu, B., Yin, K.B., Lin, J., Xia, Y. D., Wan, X.G., Yin, J., Bai, X. J., Du, J., & Liu, Z. G. (2009). Room-temperature ferromagnetism and ferroelectricity in Fe-doped $BaTiO_3$. *Physical Review B-Condensed Matter and Materials Physics, 79*(13), 2–6.

39. Deka, B., Ravi, S., Perumal, A., & Pamu, D. (2014). Ferromagnetism and ferroelectricity in Fe doped $BaTiO_3$. *Physica B: Condensed Matter, 448*(1), 204–206.

40. Lin, F., Jiang, D., Ma, X., & Shi, W. (2008). Effect of annealing atmosphere on magnetism for Fe-doped $BaTiO_3$ ceramic. *Physica B: Condensed Matter, 403*(17), 2525–2529.

41. Maier, R. & Cohn, J. L. (2002). Ferroelectric and ferrimagnetic iron-doped thin-film $BaTiO_3$: Influence of iron on physical properties. *Journal of Applied Physics, 92*(9), 5429–5436.

42. Valant, M., Arčon, I., Mikulska, I., & Lisjak, D. (2013). Cation order–disorder transition in Fe-doped 6H-$BaTiO_3$ for dilute room-temperature ferromagnetism. *Chemistry of Materials, 25*(17), 3544–3550.

43. Mikulska, I., Valant, M., Arčon, I., & Lisjak, D. (2015). X-ray absorption spectroscopy studies of the room-temperature ferromagnetic Fe-doped 6H-$BaTiO_3$. *Journal of the American Ceramic Society, 98*(4), 1156–1161.

44. Rajamani, A., Dionne, G. F., Bono, D., & Ross, C. A. (2005). Faraday rotation, ferromagnetism, and optical properties in Fe-doped $BaTiO_3$. *Journal of Applied Physics, 98*(6), 2–6.

45. Ray, S., Mahadevan, P., Mandal, S., Krishnakumar, S. R., Kuroda, C. S., Sasaki, T., Taniyama, T., & Itoh, M. (2008). High temperature ferromagnetism in single crystalline dilute Fe-doped $BaTiO_3$. *Physical Review B-Condensed Matter and Materials Physics, 77*(10), 1–6.
46. Liu, H., Cao, B., & O'Connor, C. (2011). Intrinsic magnetism in $BaTiO_3$ with magnetic transition element dopants (Co, Cr, Fe) synthesized by sol-precipitation method. *Journal of Applied Physics, 109*(7), 1–4.
47. Wei, X. K., Su, Y. T., Sui, Y., Zhang, Q. H., Yao, Y., Jin, C. Q., & Yu, R. C. (2011). Structure, electrical and magnetic property investigations on dense Fe-doped hexagonal $BaTiO_3$. *Journal of Applied Physics, 110*(11), 1781–1786.
48. Kaur, J., Kotnala, R. K., & Verma, K. C. (2011). Multiferroic properties of $Ba(Fe_xTi_{1-x})O_3$ nanorods. *Materials Letters, 65*(19–20), 3160–3163.
49. Wei, X. K., Zou, T., Wang, F., Zhang, Q. H., Sun, Y., Gu, L., Hirata, A., Chen, M. W., Yao, Y., Jin, C. Q., & Yu, R. C. (2012). Origin of ferromagnetism and oxygen-vacancy ordering induced cross-controlled magnetoelectric effects at room temperature. *Journal of Applied Physics, 111*(7), 073904.
50. Mishra, A., & Mishra, N. (2012). Iron-doped $BaTiO_3$: Influence of iron on physical properties. *International Journal of Materials Science and Applications, 1*(1), 14-22.
51. Verma, K. C., Gupta, V., Kaur, J., & Kotnala, R. K. (2013). Raman spectra, photoluminescence, magnetism and magnetoelectric coupling in pure and Fe doped $BaTiO_3$ nanostructures. *Journal of Alloys and Compounds, 578,* 5–11.
52. Maikhuri, N., Panwar, A. K., & Jha, A. K. (2013). Investigation of A- and B-site Fe substituted $BaTiO_3$ ceramics. *Journal of Applied Physics, 113*(17), 15–18.
53. Venkata Ramana, E., Yang, S. M., Jung, R., Jung, M. H., Lee, B. W., & Jung, C. U. (2013). Ferroelectric and magnetic properties of Fe-doped $BaTiO_3$ thin films grown by the pulsed laser deposition. *Journal of Applied Physics, 113*(18), 187219-1–187219-4.
54. Guo, Z., Yang, L., Qiu, H., Zhan, X., Yin, J., & Cao, L. (2012). Structural, magnetic and dielectric properties of Fe-doped $BaTiO_3$ solids. *Modern Physics Letters B, 26*(09), 1250056.
55. Dietl, T., Ohno, H., Matsukura, F., Cibert, J., & Ferrand, D. (2000). Zener model description of ferromagnetism in zinc-blende magnetic semiconductors. *Science, 287*(5455), 1019–1022.
56. Coey, J. M .D., Venkatesan, M., & Fitzgerald, C. B. (2005). Donor impurity band exchange in dilute ferromagnetic oxides. *Nature Materials, 4*(2), 173–179.

57. Chakraborty, T., Meneghini, C., Aquilanti, G., & Ray, S. (2013). Microscopic distribution of metal dopants and anion vacancies in Fe-doped $BaTiO_{3-\delta}$ single crystals. *Journal of Physics Condensed Matter, 25*(23), 236002.

58. Zorko, A., Pregelj, M., Gomilšek, M., Jagličić, Z., Pajić, D., Telling, M., Arčon, I., Mikulska, I., & Valant, M. (2015). Strain-induced extrinsic hhigh-temperature ferromagnetism in the Fe-doped hexagonal barium Titanate. *Scientific Reports, 5,* 1–7.